A New Approach for Modelling Simultaneous Storage and Growth Processes for Activated Sludge Systems Under Aerobic Conditions

Gürkan Sin,[1] Albert Guisasola,[2] Dirk J. W. De Pauw,[1] Juan A. Baeza,[2] Julián Carrera,[2] Peter A. Vanrolleghem[1]

[1]BIOMATH, Department of Applied Mathematics, Biometrics and Process Control, Ghent University, Coupure Links 653, B-9000 Gent, Belgium; telephone: +32 9 264 59 37; fax: +32 9 264 62 20; e-mail: gurkan@biomath.ugent.be
[2]Departament d'Enginyeria Química, ETSE, Universitat Autònoma de Barcelona, Bellaterra (Barcelona), Spain

Abstract: By critically evaluating previous models, a new mechanistic model is developed to describe simultaneous storage and growth processes occurring in activated sludge systems under aerobic conditions. Identifiability was considered an important criterion during the model development since it among others helps to increase the realiability and applicability of models to full-scale WWTPs. A second order model was proposed for description of the degradation of the storage products under famine conditions. The model is successfully calibrated by only using OUR data obtained from batch experiments. Calibrations were performed with biomass from full-scale WWTPs in Belgium and Spain. Predictions of the calibrated model were successfully confirmed using off-line PHB measurements, supporting the validity of the model. An iterative experimental design procedure was successfully applied and found to remarkably improve the parameter estimation accuracy for the growth on storage parameters K_1 and K_2, which used to have large confidence intervals when using standard experiments. The estimated biomass growth yield on substrate (0.58 mgCOD/mgCOD) is quite close to the theoretically expected range for heterotrophic growth. This became possible by properly accounting for the storage process. Moreover, the maximum growth rate was predicted in the range 0.7–1.3 per day. This range, albeit quite lower than the values reported for the growth-based ASM models, is believed to be more realistic. Finally, the new model is expected to better and more mechanistically describe simultaneous storage and growth activities of activated sludge systems and as such could contribute to improved design, operation and control of those systems. © 2005 Wiley Periodicals, Inc.

Keywords: activated sludge modelling; storage metabolism; respirometry; practical identifiability; optimal experimental design (OED)

INTRODUCTION

The modelling of activated sludge processes, particularly the biological substrate conversions, has evolved fundamentally in the last two decades from simple growth-based kinetics (ASM1, Henze et al., 2000) to more complicated models involving the description of storage phenomena (Gujer et al., 1999). The major driving force behind this modelling trend was the increased understanding of storage polymers to be an essential intermediate in the overall substrate removal in (full-scale) activated sludge systems, particularly subjected to feast and famine conditions (Beccari et al., 2002; Beun et al., 2000; Carucci et al., 2001; Dircks et al., 2001; Henze et al., 2000; Krishna and van Loosdrecht, 1999; Pratt et al., 2004; van Loosdrecht et al., 1997).

ASM3 is one of the first models to address the storage phenomenon. To keep the modelling exercise simple (Gujer et al., 1999), it assumed that all readily biodegradable substrate (S_S) is first stored as internal storage products (X_{STO}) before it is used for growth during the famine phase. Being the first attempt to evaluate ASM3 using experimental data, Krishna and van Loosdrecht (1999) had observed that ASM3 failed to model two significant experimental observations: (i) the discontinuity in the growth rate of biomass observed experimentally in feast and famine phases and (ii) it required prediction of higher levels of internal storage polymers than measured to fit the oxygen consumption during feast and famine phases.

The major reason of this failure was the experimentally observed fact that storage and growth occur simultaneously during the feast phase as opposed to the assumption of ASM3 that only storage occurs during the feast phase (Beun et al., 2000; Krishna and van Loosdrecht, 1999; van Aalst-van Leeuwen et al., 1997). This fact led to the formulation of the first simultaneous storage and growth model to better interpret the experimental data by Krishna and van

Loosdrecht (1999). Guisasola et al. (2004b), moreover, showed that the ASM3 approach also causes severe practical identifiability problems that resulted in unrealistic and non-mechanistic parameter estimates when using batch OUR data, the traditional way in model calibration. From a mechanistic modelling point of view, it becomes clear that ASM3 should be extended to account for simultaneous storage and growth. In addition to Krishna and van Loosdrecht (1999), several models have been proposed to improve the mechanistic modelling of simultaneous storage and growth processes in activated sludge systems (see below). However, there is no commonly agreed model yet.

This research aims to further improve the understanding and mechanistic modelling of simultaneous storage and growth processes occurring in activated sludge systems with slowly growing biomass under low F/M in view of modelling full-scale WWTPs. To this aim, a new model is developed by critically evaluating previously proposed models for feast and famine conditions. A particular emphasis is given to the kinetic description of the degradation of storage polymers under famine conditions for biomass with low PHB content, as typically found in full-scale WWTPs. To facilitate full-scale application of the model, the aim also includes the development of a simple calibration methodology only based on batch OUR data. The model is applied to batch OURs obtained with biomass sampled from two WWTPs in Belgium and Spain respectively. Practical identifiability analysis of the model parameters is performed to gain better insight into the model structure in view of improving the parameter estimation procedure. Finally, optimal experimental design (OED) is used as a tool to improve parameter estimation accuracy using OUR measurements alone.

MATERIALS AND METHODS

Experimental Set-Up

Experiment A was performed using the hybrid-respirometric set-up described in Sin et al. (2003). During this experiment, the pH was fixed at 7.80 ± 0.03 using a pH controller and the resulting acid addition profile was recorded (Gernaey et al., 2002a). Experiments B were performed in a 10 L reactor operated as an LFS type respirometer (Spanjers et al., 1998), which was developed in a previous work (Guisasola et al., 2004a). PHB was measured according to the modified method of Comeau et al. (1988) as described in Guisasola et al. (2004a).

In both set-ups, the biomass was first aerated overnight to reach an endogenous state. Then, a first pulse of acetate was added to induce a 'wake-up' effect on the biomass activity (Vanrolleghem et al., 1998). At the same time, ammonia in excess and ATU (30 mg/L) were added to avoid growth-limitation and nitrification respectively. Activated sludge sampled from two different WWTPs was used during the experimental work: Experiment A used biomass from the Ossemeersen WWTP (Gent, Belgium) whereas Experiment B used biomass from Granollers WWTP (Catalonia, Spain).

Both WWTPs perform COD removal, nitrification and denitrification. These biomass samples were analysed for TSS and VSS according to Standard Methods (APHA, 1995).

Parameter Estimation and Confidence Intervals

Modelling, simulation and parameter estimation were performed using MATLAB 6.5 (The MathWorks, Natick, MA). The differential equations were solved using an explicit Runge–Kutta (4,5) formula. Parameter estimation was carried out by using the Nelder and Mead (1965) simplex minimization algorithm. The confidence intervals of parameter estimates were determined using the inverse of the Fisher information matrix (FIM):

$$\text{FIM} = \sum_{k=1}^{N} Y_\theta^T(t_k) Q_k Y_\theta(t_k) \qquad (1)$$

$$\text{COV}(\theta_0) \geq \frac{1}{\text{FIM}} \qquad (2)$$

where $Y_\theta(t)$ is the so called output sensitivity function and Q_k is the inverse of the covariance matrix of the measurement noise (Dochain and Vanrolleghem, 2001).

MODEL DEVELOPMENT

Feast Phase

Modelling simultaneous storage and growth consists of two distinct but complementary phases: feast and famine. Under feast conditions, two modelling approaches have been employed: traditional ASM and metabolic approaches. In the first approach based on a traditional ASM-type model structure, three distinctive yield coefficients independent from each other are used for storage, direct growth on external substrate and growth on internal storage products respectively (Beccari et al., 2002; Carucci et al., 2001; Karahan-Gül et al., 2003; Krishna and van Loosdrecht, 1999; Pratt et al., 2004).

The second approach is based on the metabolic model of van Aalst-van Leeuwen et al. (1997) for pure cultures (Beun et al., 2000, 2002; van Loosdrecht and Heijnen, 2002). In this metabolic model, it has been demonstrated that the yield coefficients of storage, direct growth on substrate and growth on internal storage products respectively are linked to each other through metabolism of the substrate. Further, the yield coefficients are observed to depend on the efficiency of the oxidative phosphorylation (δ), i.e. the efficiency of energy (ATP) generation in cells (Beun et al., 2000; van Aalst-van Leeuwen et al., 1997). This approach makes it possible to restrict the calibration to the estimation of only one parameter (δ) instead of three yield coefficients.

$$Y_{\text{H,S}} = \frac{4 \cdot \delta - 2}{4.2 \cdot \delta + 4.32} \times \frac{4.2}{4}; \; Y_{\text{STO}} = \frac{4 \cdot \delta - 2}{4.5 \cdot \delta} \times \frac{4.5}{4}$$

$$\text{and } Y_{\text{H,STO}} = \frac{4.5 \cdot \delta - 0.5}{4.2 \cdot \delta + 4.32} \times \frac{4.2}{4.5} \qquad (3)$$

where $Y_{H,S}$ is the growth yield on substrate (mgCOD-X/mgCOD-S), Y_{STO} is the storage yield on substrate (mgCOD-STO/mgCOD-S) and $Y_{H,STO}$ is the growth yield on storage products (mgCOD-X/mgCOD-STO).

Kinetic Modelling of Substrate Flux Under Feast Phase

Studies of the storage phenomenon with pure cultures at low SRT's (i.e. high growth rate) showed that storage is dependent on the growth rate of the culture (van Aalst-van Leeuwen et al., 1997). In other words, the accumulation rate of storage products was linearly correlated to the difference between the maximum substrate uptake rate and the substrate uptake rate required for growth. When the culture is operated at a growth rate close to its maximum substrate uptake rate, negligible storage is observed.

On the other hand, most WWTPs are typically operated at high SRT's (i.e. low growth rate) to achieve complete biological nutrient removal resulting in biomass with a rather low average growth rate (∼1/SRT). In these systems, it is hypothesized that the maximum substrate uptake rate (q_{MAX}) of the biomass is higher than the amount needed for the average growth rate. Consequently, the maximum substrate flux into the cell exceeds the amount used for the maximum growth of the biomass and the difference is diverted to formation of the storage polymers. In this range, the q_{MAX} is slightly changing with SRT while μ_{max} is strongly affected by SRT variation (van Loosdrecht and Heijnen, 2002). Since the storage becomes the dominant process under these conditions, the ratio of PHB produced per acetate taken up can be considered constant as was confirmed experimentally (Beun et al., 2000, 2002; Dircks et al., 2001; etc.).

From a mathematical point of view, the biological control of substrate flux into the cell can be illustrated using a branch-pipe analogy (see Fig. 1). In the branch-pipe analogy, the flow $F1$ stands for the substrate influx into the cell (substrate uptake rate), $F3$ for the substrate flux diverted to growth and $F2$ for the substrate flux diverted to storage. Experimental observations show that the ratio of storage products to substrate taken up ($F2/F1$) is constant around a certain value (e.g. 0.67 gCOD/gCOD; van Loosdrecht and Heijnen, 2002). The remaining substrate flux is diverted to growth ($F3$). This experimental observation can be modelled by considering a ratio controller on the flow $F2$ that is indicated by valve A. In

this way, the flow of $F2$ can be controlled by fixing its value to a certain fraction of $F1$, f_{STO} (i.e., $F2 = f_{STO} \times F1$) which means that the substrate flow to $F3$ is also controlled at ($F1 - F2 = F3$; $F3 = (1 - f_{STO}) \times F1$).

From a *strict* mathematical point of view, it is not important where the control valve is allocated to allow for a good description of the experimental observations. However, it may have two different meanings. Most probably the reality consists of a mixture of biomass with different strategies, but this is beyond the scope of this study. However, the mathematical representation of both strategies remains largely the same. Consequently, the substrate flux under feast conditions can be modelled as follows:

$$r_S^{IN} = r_S - \frac{1}{Y_{HS}} r_{XH} - \frac{1}{Y_{STO}} r_{STO} \qquad (4)$$

The internal substrate concentration, S_S^{IN}, is assumed at steady state (i.e. $r_S^{IN} = 0$). The steady state assumption of S_S^{IN} is mostly correct during the feast phase, except for the two short unsteady-state/transient phases occurring in a pulse experiment: (i) at the time of S_S pulse addition and (ii) just after depletion of S_S respectively. The description of the first unsteady-state part can be lumped into the description of the transient response usually observed in batch experiments (Vanrolleghem et al., 2004). The second unsteady-state phase will be captured by a small change in the substrate affinity constant (K_S). Therefore, for most of the time:

$$r_S = \frac{1}{Y_{H,S}} r_{XH} + \frac{1}{Y_{STO}} r_{STO} \qquad (5)$$

Equation 5 can be translated into the following equality (assuming no substrate limitations in Eq. 5):

$$q_{MAX} = \frac{\mu_{MAX,S}}{Y_{H,S}} + \frac{k_{STO}}{Y_{STO}} \qquad (6)$$

Based on experimental observations of the constant ratio of substrate uptake/storage as discussed above in detail, the control is assumed on $F2$ which means that biomass is maximising storage rate (see above):

$$k_{STO} = f_{STO} \cdot q_{MAX} \cdot Y_{STO} \text{ and}$$
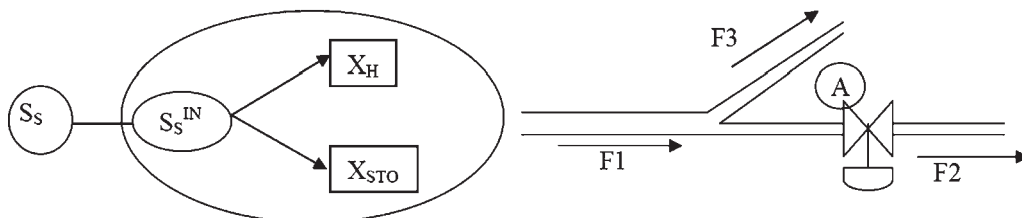$$\mu_{MAX,S} = (1 - f_{STO}) \cdot q_{MAX} \cdot Y_{H,S} \qquad (7)$$

Figure 1. Illustration of substrate flux into the cell (**left**) and branch-pipe analogy for control of substrate flux under feast conditions (**right**) (see text for explanation).

where f_{STO} is the fraction of the substrate flux diverted to the storage products (mgCOD-STO/mgCOD-S). In this way, modelling the rates of simultaneous storage and growth reduces to estimation of two parameters, i.e. f_{STO} and q_{MAX}. As discussed below, this storage ratio could be around 0.67 for WWTPs operated with high SRT. However, this value should not be taken as universal, since it is influenced by many factors such as the influent wastewater composition, history of biomass, operational strategy, e.g. feast/famine ratio, the SRT, etc.

It is important to note that from a metabolic point of view Equation 6 also includes a fraction of substrate used for maintenance, i.e. the Herbert–Pirt equation (Beun et al., 2000; van Loosdrecht and Heijnen, 2002). However, in traditional ASM models (Henze et al., 2000) the maintenance concept of the biomass is already lumped into the endogenous decay coefficient describing many other processes such as death, predation, lysis etc. In this study, therefore, the maintenance of biomass is implicitly included in the endogenous decay coefficient (see Table I) in order to keep the model at a reasonable complexity.

To summarise, the choice of modelling made in this study to describe the substrate metabolism under feast conditions was (i) based on a synthesis of the conceptual backgrounds developed in the previous models (see e.g. van Aalst-van Leeuwen et al., 1997; van Loosdrecht and Heijnen, 2002; among others) and (ii) simplified to account for model identifiability concerns. The latter is a very important aspect of modelling in view of reliability and full-scale applicability of models for WWTPs (Henze et al., 2000).

Kinetic Modelling of Storage Products Under Famine Phase

It is commonly observed that degradation of the storage polymers is the rate-limiting step and as such determines the growth rate under famine conditions. However, there is no commonly agreed kinetic model yet. Two approaches have been usually employed to describe the kinetics of degradation of X_{STO} under famine conditions: surface saturation-type kinetics (Beccari et al., 2002; Henze et al., 2000; Karahan-Gül et al., 2003; Krishna and van Loosdrecht, 1999) and a first-order model (Beun et al., 2000, 2002; Dircks et al., 2001; van Aalst-van Leeuwen et al., 1997; van Loosdrecht and Heijnen, 2002).

The surface saturation-type kinetics, e.g. as in ASM3, has been shown to cause severe practical identifiability problems due to its structure, resulting in unrealistic parameter estimates (Guisasola et al., 2004b). Moreover, so far the first-order type models were developed and applied for experimental conditions leading to biomass with a high internal storage products content (Beun et al., 2002; Dircks et al., 2001). However, activated sludge from full-scale WWTPs has a much lower fraction of storage products due to the limited availability of external substrate sources as opposed to the studies in well-controlled lab environments. Hence, the first-order type kinetics may not be proper for full-scale WWTPs.

In this study several model structures including the above mentioned models have been applied to OUR data obtained with sludge from full-scale WWTPs with low PHB content (results not shown). The following kinetic expression was found to describe the degradation of storage products reasonably well:

$$f\left(\frac{X_{STO}}{X_H}\right) = \frac{\frac{X_{STO}}{X_H}}{K_{STO} + \frac{X_{STO}}{X_H}} \times \frac{\frac{X_{STO}}{X_H}}{f_{XSTO}^{REG}} \quad (8)$$

In this mathematical expression, the first part describes the surface-saturation type degradation kinetics of X_{STO}— similar to the concept employed in ASM3 (Henze et al., 2000). The second part assumes that the degradation of X_{STO} is regulated as function of the storage content of the cell, $f_{XSTO} = X_{STO}/X_H$ (see Dircks et al., 2001). This means that when f_{XSTO} is high, the degradation of X_{STO} is faster, depending on the regulation constant of the cell, f_{XSTO}^{REG}.

Table I. Matrix representation of the extended ASM3 model (see text for explanation).

Processes	1. S_O g O_2	2. S_S g COD	3. S_{NH} g N	4. X_H g COD	5. X_I g COD	6. X_{STO} g COD	Kinetics
1. Formation of storage products, X_{STO}	$-\frac{1-Y_{STO}}{Y_{STO}}$	$\frac{-1}{Y_{STO}}$				1	$(1-e^{t/\tau})k_{STO} \cdot M_O \cdot M_S \cdot X_H$
2. Aerobic growth on external substrate, S_S	$-\frac{1-Y_{H_S}}{Y_{H_S}}$	$\frac{-1}{Y_{H_S}}$	$-i_{NBM}$	1			$(1-e^{t/\tau})\mu_{MAX,S} \cdot M_S M_O M_{NH} X_H$
3. Aerobic growth on storage products, X_{STO}	$-\frac{1-Y_{H_{STO}}}{Y_{H_{STO}}}$		$-i_{NBM}$	1		$-\frac{1}{Y_{H_{STO}}}$	$\mu_{MAX,STO} M_O M_{NH} \frac{\left(\frac{X_{STO}}{X_H}\right)^2}{K_2 + \frac{X_{STO}}{X_H} \cdot K_1} \cdot \frac{K_S}{S_S + K_S} X_H$
4. Endogenous respiration	$-(1-f_{XI})$		$i_{NBM}-i_{NXI}f_{XI}$	-1	f_{XI}		$b_H M_O X_H$
5. Endogenous respiration of X_{STO}	-1					-1	$b_{STO} M_O X_{STO}$
6. Aeration	1						$K_L a \cdot (S_O^* - S_O)$

$k_{STO} = f_{STO} \cdot q_{MAX} \cdot Y_{STO}$; $\mu_{MAX,S} = (1-f_{STO}) \cdot q_{max} \cdot Y_{H,S}$; M stands for a Monod kinetic function (the substrate considered is indicated in the subscript) e.g. $M_S = S_S/(K_S + S_S)$.

The first-order empirical model $(1-e^{t/\tau})$ is used to model the transient response observed in OUR data obtained from batch experiments (Guisasola et al., 2003; Vanrolleghem et al., 2004).

However, when f_{XSTO} is decreasing and approaching a minimum level in the biomass, the biomass starts to limit the degradation rate of X_{STO}. The particular reasons behind the choice of this kinetic expression are: (i) it was shown explicitly that the degradation rate of PHB strongly depends on the PHB content of the cell (Dircks et al. (2001), (ii) it was hypothesised that biomass always contains a minimum PHB content (van Aalst-van Leeuwen et al., 1997). This implies that biomass is likely to control the degradation rate of storage products such that a minimum level of storage products can be maintained, (iii) experimental observations (particularly OUR from batch experiments) showed that there are at least two phenomena corresponding to a fast and a slow degradation rate of X_{STO} under famine conditions (see below).

Equation 8 can be rewritten as follows, resulting in a second-order type kinetic expression:

$$f\left(\frac{X_{STO}}{X_H}\right) = \frac{\left(\frac{X_{STO}}{X_H}\right)^2}{K_2 + K_1 \cdot \frac{X_{STO}}{X_H}} \quad (9)$$

where $K_2 = K_{STO} \times f_{XSTO}^{REG}$ and $K_1 = f_{XSTO}^{REG}$.

In this expression, K_2 becomes the affinity of the biomass towards X_{STO}/X_H (mgCOD/mgCOD) and K_1 is nothing but the regulation constant of the biomass as function of X_{STO}/X_H (mgCOD/mgCOD).

The model developed in this study is summarised in matrix format in Table I. Similar to previous studies (e.g. van Loosdrecht and Heijnen, 2002), the growth rate of biomass on X_{STO} is assumed to occur under strictly famine conditions, i.e. a Monod inhibition function for external substrate is added to the kinetic description of r_{STO} (see Eq. 3 in Table I).

RESULTS

OUR for Monitoring Simultaneous Storage and Growth Processes

Respirometric measurements with biomass A obtained after pulse addition of a certain amount of acetate to endogenously respiring activated sludge are shown in Figure 2. Titrimetric measurements (Hp) are also shown in the same figure. In this way, one can indirectly monitor the acetate uptake from the medium (see e.g. Gernaey et al., 2002a). The monitoring principle of titrimetric measurement is that acetate is a weak acid and at pH equal to 7.8 is present in dissociated form in the medium. Therefore, its cellular uptake is accompanied by a certain amount of protons ($\sim$1 mmole H^+/1 mmole acetate) to preserve the charge balance of the cell (for further modelling details reader is referred to Gernaey et al., 2002b). Since quantitative interpretation of the titrimetric data requires a complicated model-based approach, in this study it is used only as quality check for the respirometric measurements.

Upon pulse addition of substrate, i.e. under the feast conditions, the OUR of biomass A increases gradually to a
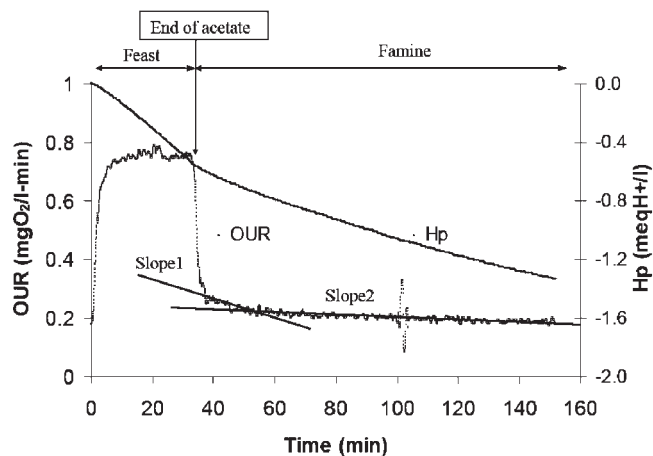

Figure 2. Oxygen uptake rate measurements after pulse addition of acetate to endogenously respiring biomass A (see text for explanation).

maximum level following a fast transient (ca. 3–4 min) (see Fig. 2). This transient period is frequently observed in OUR data obtained from batch experiments with pulse addition of substrate (Vanrolleghem et al., 2004). The biomass activity continues at this maximum level until all external substrate is taken up for storage and growth. Similarly, the Hp data shows an increased consumption of protons from the medium upon pulse addition of acetate indicating fast and linear removal of acetate from the medium. This fast consumption of protons ceases to a slower and non-linear phase in the Hp data as marked by the sharp bending point in the Hp data (see Fig. 1) indicating that the acetate was completely removed from the medium (see Gernaey et al., 2002a; Pratt et al., 2003; Sin et al., 2003). This non-linear consumption of protons after the sharp bending point is mainly, among others, due to non-linear consumption of protons by CO_2 stripping, endogenous CO_2 production due to, e.g. utilisation of X_{STO}, etc. Note that this sharp bending point in the Hp data coincides well with the sharp drop in the OUR data of biomass A (see Fig. 2). In the famine phase, the OUR of biomass A drops from the maximum level to a level higher than the endogenous OUR level maintained prior to substrate addition (see Fig. 2). Under famine conditions, biomass grows using internal storage products, X_{STO}, produced in the previous phase. A similar pattern of acetate oxidation is observed with biomass B (Fig. 3, right).

The oxygen uptake rate is observed to have two different slopes indicating two phenomena under famine conditions (see Fig. 2). This observation was the particular reason for the choice of second order kinetics for the description of the degradation of storage products (see the 'Model Development').

Calibration of the Model: Parameter Estimation Procedure

For the calibration of the model, the initial concentration of active biomass, $X_H(0)$ is estimated using the baseline
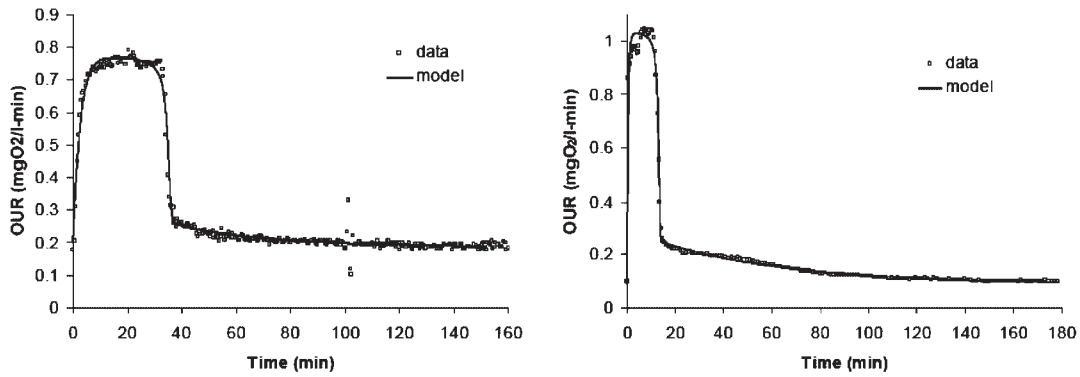
Figure 3. Model fits to the Experiment A (**left**) and Experiment B (**right**) (see Table II for the calibrated parameters). Only every 10th data point is shown to keep the figure clearer.

endogenous OUR level prior to substrate addition, while fixing the decay rate coefficient b_H to the value mentioned in the ASM models (Henze et al., 2000), i.e. 0.2 per day (see Table II). The endogenous OUR prior to substrate addition is equal to:

$$OUR_{end}(0) = (1 - f_{XI}) \cdot b_H \cdot X_H(0) \qquad (10)$$

In our approach, f_{XI} is also fixed to the value mentioned in ASM3, 0.2 mgCOD/mgCOD. From a structural identifiability point of view, it is not possible to obtain unique values of both b_H and $X_H(0)$ using short-term (e.g. 10–15 min) endogenous OUR measurements. In other words, there are an infinite number of solutions (parameter combinations of b_H and $X_H(0)$) to Equation 10. This is because the decay of biomass is practically negligible within such short-period.

Long-term (e.g. 10 days) monitoring of endogenous OUR is needed for unique estimation of b_H (Henze et al., 2000; Keesman et al., 1997). Hence, for given f_{XI} and b_H, the $X_H(0)$ can be calculated from the OUR(0) data.

Moreover, the endogenous utilisation rate of X_{STO}, b_{STO}, is taken the same as the endogenous decay rate of biomass, b_H, similar to the approach adopted in ASM3 (Henze et al., 2000).

The estimation of the initial concentration of storage products, $X_{STO}(0)$ was observed to cause severe identification problems (results not shown), i.e. it has a too large confidence interval. Therefore, the initial concentration of storage products, $X_{STO}(0)$, is either measured (in Experiment B and the OED experiment) or estimated (in Experiment A) using a step-wise procedure as explained below.

Table II. Parameter estimation results with the simultaneous storage and growth model.

Parameters	Experiment A	Confidence interval[b] (%)	Experiment B	Confidence interval[b] (%)
Parameters estimated				
q_{MAX} (per day)	1.67 ± 0.09[a]	5.39	6.43 ± 0.05[a]	0.78
f_{STO} (mgCOD/mgCOD)	0.29 ± 0.07	24.14	0.65 ± 0.09	13.85
δ (mol/mol)	2.88 ± 0.16	5.56	2.57 ± 0.22	8.56
K_S (mgCOD/L)	0.6 ± 0.4	66.67	0.67 ± 0.11	16.42
K_1 (mgCOD/mgCOD)	0.015 ± 0.029	193.33	0.053 ± 0.041	77.36
K_2 (mgCOD/mgCOD)	$1.7 \times 10^{-4} \pm 3 \times 10^{-4}$	182.35	$9.8 \times 10^{-4} \pm 1 \times 10^{-3}$	102.04
τ (min)	2.73 ± 0.12	4.40	0.51 ± 0.05	10
Parameters estimated using the step-wise procedure (see text for explanation)				
$X_{STO}(0)$ (mgCOD/L)	0.99 (estimated)		6.8 (measured)	
Parameters assumed				
b_H (per day)	0.2		0.2	
b_{STO} (per day)	0.2		0.2	
f_{XI} (mgCOD/mgCOD)	0.2		0.2	
Parameters calculated				
$X_H(0)$ (mgCOD/L)	1,650		800	
$q_{MAX} \times X_H(0)$ (mgCOD/L-d)	2,755		5,144	
$\mu_{MAX,S}$ (per day)	0.72		1.3	
k_{STO} (per day)	0.4		3.31	
$\mu_{MAX,STO}$ (per day)	0.72		1.3	
Y_{STO} (mgCOD/mgCOD)	0.83		0.81	
$Y_{H,S}$ (mgCOD/mgCOD)	0.61		0.58	
$Y_{H,STO}$ (mgCOD/mgCOD)	0.71		0.68	

[a]Parameter estimates are given together with 95% confidence interval.
[b]Confidence intervals are presented in these columns as absolute percentage of the parameter estimates, i.e. (confidence interval/parameter) × 100.

The maximum growth rate of biomass on X_{STO}, $\mu_{MAX,STO}$, is assumed to be in the same order of magnitude as the maximum growth rate of biomass on external substrate, $\mu_{MAX,S}$, in order to keep the model calibration exercise at a reasonable complexity. It is important to note that from a parameter estimation point of view, any possible error involved in this assumption is most likely compensated by the estimate of K_2 or K_1 (see Eq. 3 in Table I). The yield coefficients for storage, (Y_{STO}), direct growth on S_S, ($Y_{H,S}$) and growth on X_{STO}, ($Y_{H,STO}$) are calibrated by estimating the δ parameter using the relations given above. The maximum storage rate, k_{STO}, and the maximum growth rate of biomass, μ_{MAX}, are calculated from the estimates of the maximum substrate uptake rate, q_{MAX}, and the fraction of substrate used for storage f_{STO} using the substrate flux model described above.

Parameter Estimation Results

Parameter estimation results obtained using OUR measurements with biomass A and biomass B are summarised in Table II while best fits of the model to the experimental data are shown in Figure 3. The model fits are quite acceptable/plausible (see Fig. 3).

The ratio of substrate uptake to substrate used for storage, f_{STO}, was found low in Experiment A (for biomass A) compared to the average value 0.67 mgCOD/mgCOD reported for pure and mixed cultures sampled from systems having SRT higher than 5 days (Beun et al., 2002; van Loosdrecht and Heijnen, 2002). This implies that the mixed culture used in Experiment A has a lower storage capacity which is possibly due to the composition of biomass A being different as it has different growth strategies, i.e. direct growth on external substrate versus substrate storage followed by growth on storage product. From modelling point of view, it is noted that the extended ASM3e model is still able to well describe the OUR data in Experiment A (see Fig. 3, left) adding credibility to the range of applicability of the model. On the other hand, the storage fraction of biomass B is in good agreement with the typical value mentioned above. The substrate uptake rate of biomass A (i.e. $q_{MAX} \times X_H(0)$) is observed to be approximately half that of the substrate uptake rate of biomass B. As a result, the kinetic parameters estimated for biomass A were also slower than the kinetic parameters estimated for biomass B (see Table II).

Nonetheless, the μ_{MAX} estimates of both biomass samples are noticeably lower than the typical range of values reported in literature for the maximum heterotrophic growth rate for municipal WWTPs (Gernaey et al., 2002b; Henze et al., 2000; Vanrolleghem et al., 2004; etc.). The substrate affinity constants, K_S, of biomass A and biomass B (see Table II) were also found to be in the same order of magnitude of the values obtained from other batch experiments (Gernaey et al., 2002b; Vanrolleghem et al., 2004). The storage uptake rate, k_{STO}, was found to be faster than the maximum growth rate, μ_{MAX}, for biomass B, which is in agreement with the experimental findings of Pratt et al. (2004).

Practical Parameter Identifiability

Practical identifiability of a model structure is important as it tells which parameter combinations can be estimated under given measurement accuracy and quantity. In this way, one can improve the reliability and accuracy of the parameter estimation (Dochain and Vanrolleghem, 2001). For such identifiability study, output sensitivity functions of parameters and contour plots of the objective functional will be evaluated.

Output sensitivities of model parameters calculated using best-fit parameters obtained in Experiment B (see Table II) are shown in Figure 4. The output sensitivity function of q_{MAX} is observed to be correlated with the output sensitivity function of f_{STO} and δ during the feast phase. However, in the famine phase these correlations are broken to a large extent, thereby enabling to estimate those parameters simultaneously using OUR measurements (see Table II). The sensitivity function of K_S also has a different trajectory than that of the sensitivity of q_{MAX} unlike what happens in pure-growth models where it is often the case that μ_{MAX} is correlated with K_S (Dochain and Vanrolleghem, 2001). Moreover, the output sensitivity functions of f_{STO} and δ are also almost perfectly correlated under the feast phase but again this correlation is broken during the famine phase, making these parameters uniquely identifiable as well.

The output sensitivity functions for K_1 and K_2 are observed to be correlated until a certain time instant beyond which the correlation is broken (see Fig. 4). In this regard, the length of the famine phase becomes very important for reliable estimation of these parameters. The output sensitivities of K_1 and K_2 have no specific correlation with the sensitivity functions of q_{MAX}, f_{STO} and δ respectively. This ensures reliable estimation of parameters K_1 and K_2 from the part of data collected under famine conditions.

In summary, the output sensitivity functions of the model parameters estimated in Table II suggest that they are practically identifiable using OUR measurements alone. These results are also checked with the analysis of the shape of the cost/objective functional performed below.

The contour plots of the objective function shown in Figure 5 were calculated around the optimum for different combinations of parameters: f_{STO} and δ (Fig. 5, left) and K_1 and K_2 (Fig. 5, right). The contours of the objective function are large in both planes of the two-parameter subsets i.e. $f_{STO}-\delta$ plane and K_1-K_2 planes respectively. Particularly in the plane K_1 and K_2 (see Fig. 5, right), the objective function is observed to be valley-like in a certain direction. This means that several combinations of parameters K_1 and K_2 will give almost equally good fits to the data leading to large confidence intervals of the parameter estimates (Baltes et al., 1994; Dochain and Vanrolleghem, 2001). This is indeed observed in the parameter estimation results. The relative errors on parameter estimates K_1 and K_2 are calculated to be 77% and 102% respectively in Experiment B (see Table II). When confronted with such situation, OED has been shown
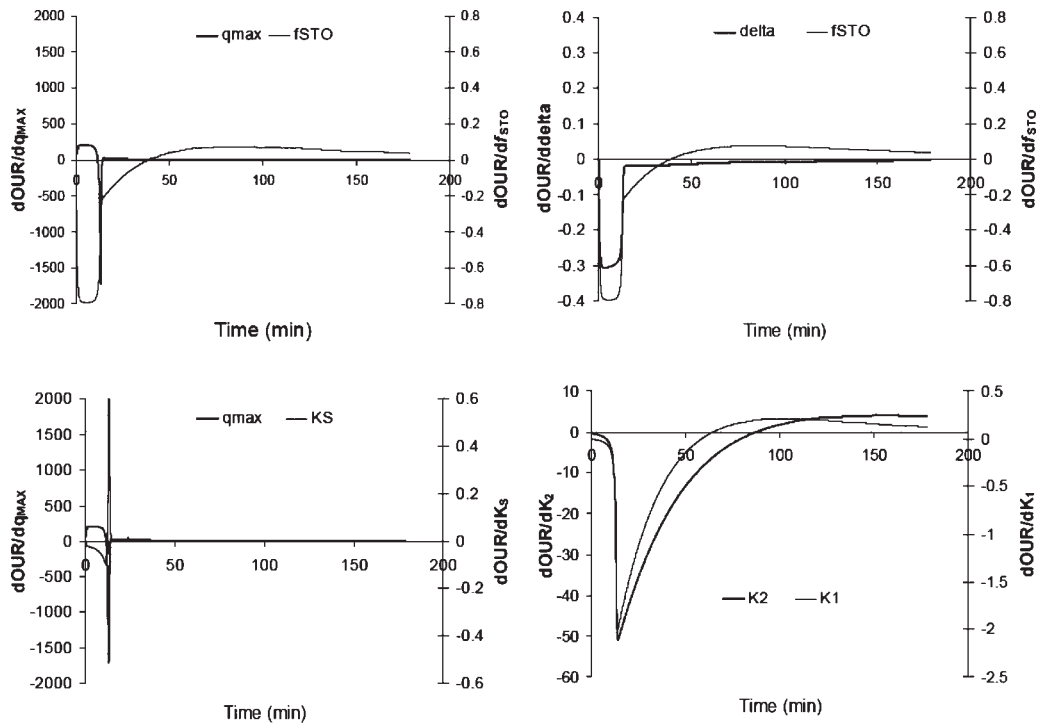
Figure 4. Output sensitivity functions of model parameters calculated around best-fit conditions for Experiment B (see text for explanation). Note that 'delta' is 'δ'.

to improve parameter estimation accuracy (Dochain and Vanrolleghem, 2001; Vanrolleghem et al., 1995).

OED for Parameter Estimation

The OED procedure presented in Dochain and Vanrolleghem (2001) is used to improve the confidence interval for parameter estimation. The reference experiment was chosen to be Experiment B. The parameter subset considered for parameter estimation consists of q_{MAX}, f_{STO}, K_1, K_2, τ, K_S and δ. The experimental degrees of freedom were chosen to be (1) single or two consecutive pulse additions of acetate, (2) amounts of first (and second) pulse additions and (3) time

instant of the second pulse addition. The duration of each experiment was fixed to 200 min. The substrate to biomass ratio, S/X, was constrained to 0.1 (mgCOD/mgCOD) in order to prevent any possible physiological change at the cellular level (Chudoba et al., 1992; Grady et al., 1996). Considering that the $X_H(0)$ was approximated as 800 mgCOD/L (see Table II), the total added substrate was fixed to 80 mgCOD/L.

An iterative OED procedure was followed. The FIM, which is the basis for OED, is calculated to summarise the information content of each hypothetical experiment under different combinations of the above-mentioned degrees of freedom (Dochain and Vanrolleghem, 2001). The D and Mod-E criteria of FIM, the most frequently used FIM
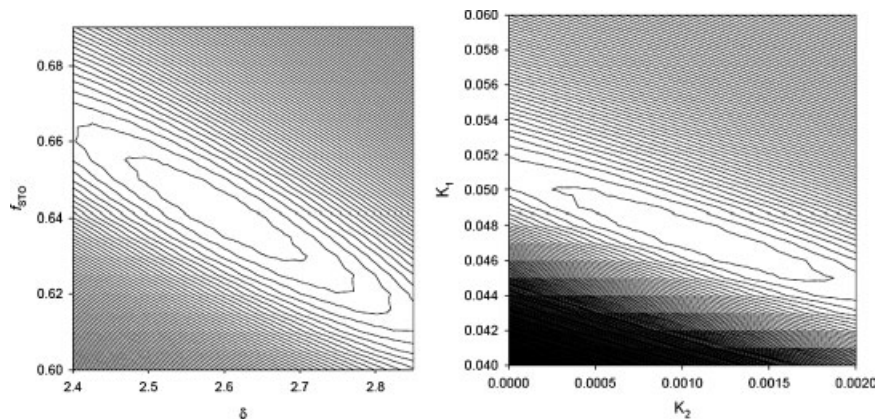

Figure 5. Contour plots of the objective functional used for parameter estimation as function of two parameters; f_{STO} and δ (**left**) and K_1 and K_2 (**right**).

properties of for optimisation of the experiment, are used in this study too (Dochain and Vanrolleghem, 2001; Vanrolleghem et al., 1995).

The results of OED under various combinations of degrees of freedom are summarised in Figure 6. The objective is to find an experiment with the lowest Mod-E and the highest D criteria values. It can be seen from Figure 6 (see the circled regions) that the optimal experiment according to the OED analysis is a two pulse addition of (40 mg COD/L each) where the second pulse is added around 20 min, which corresponds to an addition just before the first pulse of substrate is completely taken up by the biomass. This is very similar to the results of Vanrolleghem et al. (1995). The optimal experiment results in two peaks in the OUR profile,

thereby improving the accuracy of parameter estimation of the feast phase. Moreover, the parameters of the famine phase are also better estimated thanks to the increased PHB content of the cell and the elongated OUR tail thanks to the previous two pulses.

Implementation of the OED Experiment

The optimal experiment resulting from the OED study was applied to biomass B and the experimental results are shown in Figure 7, including off-line PHB measurements. Upon the first pulse addition of acetate, the OUR immediately increases to a maximum level following a fast transient. Parallel to this increase in the OUR, the PHB content of the
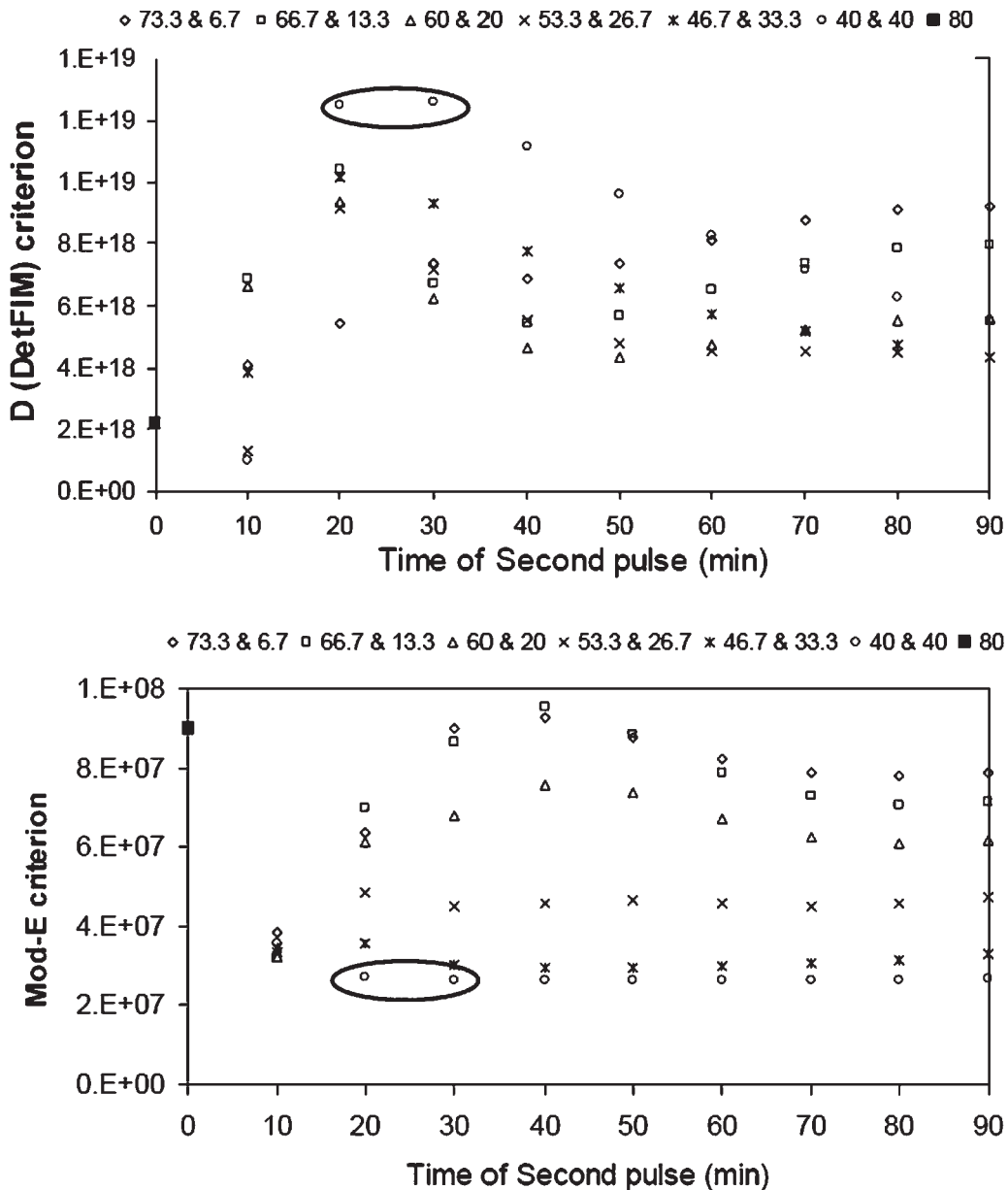

Figure 6. Properties of Fisher information matrix (FIM) as a function of the pulse time and the concentration of the pulses: D-criterion (**top**) and Mod-E criterion (**down**) (see text for explanation).
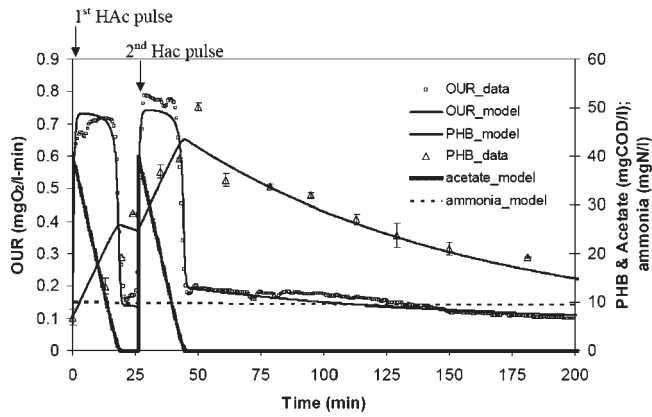
Figure 7. Implementation of the optimal experimental design (OED) experiment with two pulse additions of equal amounts of acetate (40 mgCOD/L) where the second acetate pulse is added after ca. 20 min.

biomass also increases linearly in time confirming that part of the acetate is diverted to storage while the rest is used for simultaneous growth (see Fig. 7).

After the first pulse of acetate is completely consumed by the biomass, the OUR drops immediately. The same phenomenon as in the first acetate pulse is repeated in the second pulse addition of acetate (see Fig. 7). The formation of PHB is continued with a linear increase for as long as acetate is present in the medium. After the second pulse of acetate is completely consumed by biomass, PHB starts to decrease gradually following a non-linear pattern. Concomitantly, the OUR is also decreased and follows a non-linear uptake rate due to the oxygen uptake for biomass growth on PHB.

The parameter estimation results for the OED experiment by only using OUR measurements are shown in Table III. It is important to stress that the PHB measurements were not used for model calibration, but instead they are compared with the predictions of the model calibrated using OUR measurements alone (Fig. 7). The model predictions for PHB are in agreement with the measured PHB content during the two consecutive pulse additions of acetate. Moreover, the model fit to the OUR measurements is acceptable. However, the model was unable to perfectly fit the second peak in the OUR profile. This is discussed below (see "Discussion").

From a parameter estimation point of view, a remarkable improvement in parameter estimation accuracy was obtained from the OED experiment (compare Tables II and III). Particularly the huge confidence intervals of K_1 and K_2 (see Table II) could be reduced from 77% and 102% to 12% and 25% respectively. In this regard, the application of the OED methodology for improving parameter estimation accuracy is clearly valuable.

Although the confidence intervals of the parameter estimates have been significantly reduced in the OED experiment, the parameter estimates themselves did not vary significantly compared to the values obtained in the reference experiment (i.e. Experiment B). For instance, the estimate of δ remained quite close to the value estimated in the reference

Table III. Parameter estimation results for the optimal experimental design (OED) experiment using only OUR data.

Parameters	OED experiment	Confidence interval[b] (%)
Parameters estimated		
q_{MAX} (per day)	4.27 ± 0.03[a]	0.70[b]
f_{STO} (mgCOD/mgCOD)	0.60 ± 0.03	5.00
δ (mol/mol ATP)	2.56 ± 0.08	3.13
K_S (mgCOD/L)	0.70 ± 0.1	14.29
K_1 (mgCOD/mgCOD)	0.102 ± 0.012	11.76
K_2 (mgCOD/mgCOD)	$1.2 \times 10^{-3} \pm 3 \times 10^{-4}$	25
τ (min)	0.51 ± 0.07	13.73
Parameters measured		
$X_{STO}(0)$ (mgCOD/L)	6.8	
Parameters assumed		
b_H (per day)	0.20	
b_{STO} (per day)	0.20	
f_{XI} (mgCOD/mgCOD)	0.20	
Parameters calculated		
$X_H(0)$ (mgCOD/L)	800.00	
$\mu_{MAX,S}$ (per day)	0.97	
k_{STO} (per day)	2.02	
$\mu_{MAX,STO}$ (per day)	0.97	
Y_{STO} (mgCOD/mgCOD)	0.80	
$Y_{H,S}$ (mgCOD/mgCOD)	0.57	
$Y_{H,STO}$ (mgCOD/mgCOD)	0.68	

[a]Parameter estimates are given together with 95% confidence interval.
[b]Confidence intervals are presented in these columns as absolute percentage of the parameter estimates, i.e. (confidence interval/parameter) × 100.

experiment (see Tables II and III). However, the estimate of q_{MAX} was found lower than the value estimated in the reference experiment (see Tables II and III) indicating that in the OED experiment biomass may have not yet reached its maximum substrate uptake rate. Since q_{MAX} was lower, the $\mu_{MAX,S}$, k_{STO} and $\mu_{MAX,STO}$ were also calculated to be lower compared to the reference experiment (compare Tables II and III). A possible explanation for this observation could be physiological adaptation as discussed below.

Finally, it was observed experimentally that the amount of substrate used for the PHB formation per amount of acetate consumed, f_{STO}, is equal to 0.68 mgCOD/mgCOD (assuming the storage yield is 0.80), which is quite close to the estimated value for f_{STO}, 0.60 mgCOD/mgCOD (see Table III). Moreover, both measured and estimated values fall in the range reported by Beun et al. (2002) for aerobic, slowly growing activated sludge cultures. This result supports the validity of the model as well as the calibration procedure using OUR measurements alone.

DISCUSSION

The Model Performance: Parameter Estimation Results

The low estimates found for the maximum growth rate, μ_{MAX}, of both biomass samples is believed to be a more realistic predictions of the true growth rate of activated

sludge in municipal WWTPs, since the storage was properly accounted for in this study. Further, the estimated maximum substrate uptake rate of biomass is much higher than the amount used for the maximum growth rate of biomass (see Table II) which supports the hypothesis that activated sludge grows slower than what the substrate uptake rate allows (Beun et al., 2002; van Loosdrecht and Heijnen, 2002).

The efficiency of the oxidative phosphorylation, (δ), was found in the theoretically expected range i.e. $1-3$ mol/mol for both biomass samples (Beun et al., 2000). Moreover, the yield coefficients calculated using the estimated δ for biomass A and biomass B were very similar even though biomass A and biomass B have different growth and storage kinetics. This result supports the validity of the proposed model structure, which assumes that the macroscopic yield coefficients are independent of the growth rate, and can be estimated using a metabolic relation (see 'Model Development'; Beun et al., 2000; van Loosdrecht and Heijnen, 2002).

The second order model adopted in this study to describe the utilisation of storage products under famine conditions fitted the OUR tail under famine conditions well. The parameter K_2, defined as the affinity of biomass as function of the storage content of biomass, X_{STO}/X_H, was found to be low for both biomass. Moreover, the traditional affinity constant of biomass to storage products, K_{STO}, calculated as K_2/K_1 (see 'Model Development'), was found around 0.01 mgCOD/mgCOD which is in agreement with the value mentioned for PAOs in ASM2d (Henze et al., 2000). Moreover, Koch et al. (2000) estimated for K_{STO} a value of 0.1 mgCOD/mgCOD using the ASM3 model. The estimated K_{STO} value in this study is significantly lower than the default value proposed for K_{STO} in ASM3 (1.0 mgCOD/mgCOD, Henze et al. (2000)). The high value of ASM3 is probably due to the severe parameter correlations of K_{STO} with the maximum growth rate of biomass (Guisasola et al., 2004b). The parameter K_1 defined as the regulation constant of biomass controlling the degradation of the storage product, was observed to change from one experiment to another experiment, making it difficult to comment on. This variability is most probably due to the problems of practical

identifiability encountered with the estimation of these two parameters K_2 and K_1 (see Fig. 5). One way to improve the identifiability of this parameter is to apply an OED methodology, as done in this study for the biomass B. Another way of improving the identifiability of these parameters is naturally to use PHB measurements for parameter estimation on top of the OUR data. It is clear that further experiences are needed in this direction.

Direct biomass growth on substrate (acetate) can be compared with the biomass production based on internally stored PHB using the following ratio $\frac{Y_{STO} \times Y_{H,STO}}{Y_{H,S}}$. This ratio is calculated to be ca. 0.96 both for biomass A and biomass B. This means that there is negligible reduction of the overall yield when PHB is used for growth, which is in agreement with the findings of Beun et al. (2000).

Practical Identifiability of the Model

Estimation of $X_{STO}(0)$ was observed to cause severe parameter identification problems when OUR is used alone. To understand the reason of this difficulty, the objective functional was calculated as a function of $f_{XSTO}(0)$ (i.e. the storage fraction of biomass expressed as $100 \times X_{STO}(0)/X_H(0)$), δ and f_{STO}. The contour plots of the objective function in both planes i.e. $f_{XSTO}(0)-\delta$ and $f_{XSTO}(0)-f_{STO}$ are large and have a valley-like shape with a very flat bottom (see Fig. 8). This shape is known to cause severe problems to optimisation algorithms in finding the minimum (Dochain and Vanrolleghem, 2001). Moreover, large contour plots of the objective functional indicate that there are many combinations of parameters that give an almost equally good fit to the measurements. This implies that the confidence intervals of the parameter estimates would also be very large. In short, the analysis of the shape of the objective functional implies that the simultaneous estimation of parameters $f_{XSTO}(0)$ (and $X_{STO}(0)$), δ and f_{STO} is difficult.

To resolve this issue the $f_{XSTO}(0)$ should be fixed to either a measured value or by using step-wise parameter estimation (Dochain and Vanrolleghem, 2001). This step-wise parameter
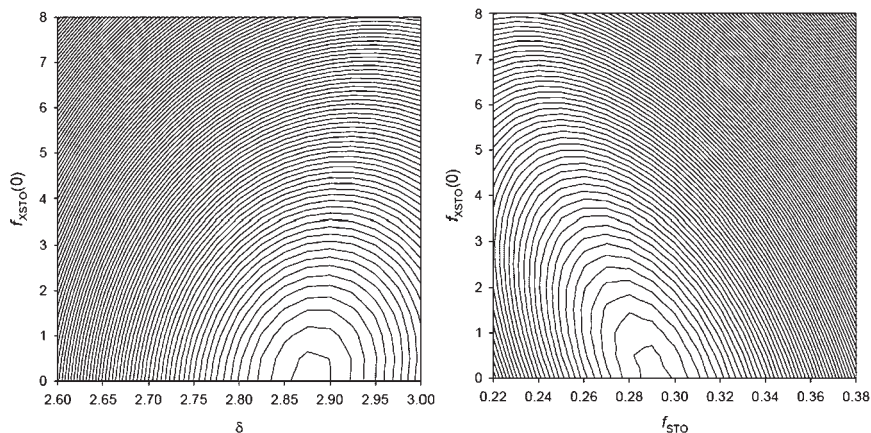

Figure 8. Contour plots of the objective functional as a function of two parameters $f_{XSTO}-\delta$ (**left**) and $f_{XSTO}-f_{STO}$ (**right**).

estimation procedure is already explained above (see calibration of the model).

Implementation of OED for Parameter Estimation

The application of the OED methodology was observed to provide remarkable improvements to the parameter estimation accuracy (compare Tables II and III). For instance, it was possible to reduce the large confidence intervals of the parameters K_1 and K_2 from 77% and 102% to 12% and 25% respectively.

However, the model could not perfectly describe the second peak in the OUR profile corresponding to the second acetate pulse (see Fig. 7). This discrepancy may be due to the not modelled physiological adaptation of the biomass. In other words, after the first pulse of acetate, the biomass increases its RNA and protein content and activity to sustain a higher growth rate (Lavallée et al., 2005; Vanrolleghem et al., 1998; van Loosdrecht and Heijnen, 2002). In this respect, it is also important to note that parameter estimates with the OED experiment remained close to the ones of the reference experiment except q_{MAX}, which was found lower than the reference experiment. This supports the above-mentioned hypothesis that the biomass in the OED experiment undergoes a transient to increase its substrate uptake rate until it reaches the maximum substrate uptake, see e.g. the q_{MAX} obtained in the reference experiment. Similar phenomena were reported and discussed in detail in Vanrolleghem et al. (1998). Since the model developed in this study aims at modelling stable activated sludge cultures for WWTPs, the 10% increase in maximum OUR can be considered negligible in view of model calibration purposes.

Implications to Full-Scale WWTP Modelling

Ultimately this research aims to extend ASM3 by critically considering previous attempts to better describe the aerobic heterotrophic growth in full-scale WWTPs in a mechanistically sound way. The model developed in this study has been applied successfully to OUR data obtained from short-term batch experiments. Like previous models, the developed model allows for separating *explicitly* substrate uptake kinetics from growth kinetics to better describe aerobic carbon oxidation processes in full-scale WWTPs but considering a compromise between model complexity and practical applicability. To this end, a particular emphasis was also given to develop a practical and easy calibration methodology based only on OUR data to facilitate the full-scale application of this type of activated sludge models.

It is expected that improved mechanistic modelling of biological processes in WWTPs will deliver a better insight into the system, which can be used to improve design, operation and control of the biological processes. Since most of the WWTPs also operate under anoxic conditions it is important to extend the model developed here to describe simultaneous storage and anoxic growth for full-scale WWTPs. This extension is done in Sin (2004).

CONCLUSIONS

In this study, the ASM3 model was successfully extended to describe simultaneous storage and growth activities of activated sludge under aerobic conditions. Modelling the substrate metabolism under feast conditions was done by synthesising previous experiences and models in view of adequate model complexity. For the famine conditions, a second-order type kinetics expression was developed to describe the degradation of storage products.

In view of facilitating full-scale application of the model, a practical calibration procedure only requiring OUR data obtained from batch experiments was developed and applied successfully to calibrate the model. The predictions of the calibrated model were also confirmed by independent PHB measurements, supporting the validity of the model. The OED methodology was shown to be valuable in view of improving the parameter estimation accuracy, particularly for the identification of the second-order model developed in this study.

The maximum growth rate of heterotrophs was estimated to be between 0.7 and 1.3 per day for the sludge tested which is quite lower compared to the values reported in literature for the growth-based ASM models. The estimated yield coefficient for heterotrophic growth on acetate was around 0.58 mgCOD/mgCOD, lower than the values reported in literature for growth-based models. It is believed that the proposed model gives a better prediction of the growth yield and the maximum growth rate of biomass in full-scale WWTPs since it accounts for the storage phenomenon. Finally, the estimated maximum substrate uptake rate of the biomass was much higher than the substrate usage rate at the maximum growth rate of the biomass.

NOMENCLATURE

ASM	activated sludge model
ASM3	activated sludge model number 3
b_H	endogenous decay coefficient of biomass, per day
b_{STO}	endogenous decay of storage products per day
COV	covariance matrix
δ	efficiency of oxidative phosphorylation, mol/mol
FIM	Fisher information matrix
f_{XSTO}^{REG}	regulation constant of biomass controlling degradation rate of X_{STO} as function of f_{XSTO}, mgCOD-X_{STO}/mgCOD-X_H
$f_{XSTO}(0)$	initial fraction of X_{STO} in biomass i.e. $X_{STO}(0)/X_H(0)$, mgCOD-X_{STO}/mgCOD-X_H
f_{XSTO}	fraction of X_{STO} in biomass i.e. $X_{STO}(0)/X_H(0)$, mgCOD-X_{STO}/mgCOD-X_H
f_{STO}	fraction of substrate used for storage, mgCOD-X_{STO}/mgCOD-S_S
$F1$	substrate influx to the cell (substrate uptake), mgCOD/L-d
$F2$	substrate flux used for storage, mgCOD/L-d
$F3$	substrate flux used for growth, mgCOD/L-d
Hp	proton concentration in mixed liquor (meq H^+/L)
K_S	substrate affinity constant, mgCOD/L
K_{STO}	biomass affinity constant for X_{STO}, mgCOD/L

K_1	regulation constant of biomass controlling degradation rate of X_{STO} as function of f_{XSTO}, mgCOD-X_{STO}/mgCOD-X_H
K_2	a lumped parameter related to the affinity of biomass to storage fraction of biomass i.e. f_{STO}, mgCOD-X_{STO}/mgCOD-X_H
k_{STO}	maximum storage rate of biomass, per day
$\mu_{MAX,S}$	maximum growth rate of biomass on substrate, per day
$\mu_{MAX,STO}$	maximum growth rate of biomass on storage products, per day
OUR	oxygen uptake rate, mgO$_2$/L-min
PHB	poly-β-hydroxybutyrate, mgCOD/L
q_{MAX}	maximum substrate uptake rate, per day
r_S	substrate uptake rate, mgCOD/L-d
r_{XH}	growth rate, mgCOD/L-d
r_{STO}	storage rate, mgCOD/L-d
S_S^{IN}	internal substrate concentration, mgCOD/L
S/X	substrate to biomass ratio, mgCOD/mgCOD
SRT	sludge residence time (d)
τ	first order time constant, min
$X_{STO}(0)$	initial concentration of storage polymers/products in biomass, mgCOD/L
$X_H(0)$	initial concentration of biomass, mgCOD/L
Y_{STO}	yield coefficient for storage on substrate, mgCOD-X_{STO}/mgCOD-S_S
$Y_{H,S}$	yield coefficient for growth on substrate, mgCOD-X_H/mgCOD-S_S
$Y_{H,STO}$	yield coefficient for growth on storage products, mgCOD-X_H/mgCOD-X_{STO}
WWTP	wastewater treatment plant

References

APHA. 1995. Standard methods for the examination of water and wastewater, 19th edn. Washington, DC: American Publishers Health Association.

Baltes M, Scheider R, Sturm C, Reuss M. 1994. Optimal experimental design for parameter estimation in unstructured growth models. Biotechnol Prog 10:480–488.

Beccari M, Dionisi D, Giuliani A, Majone M, Ramadori R. 2002. Effect of different carbon sources on aerobic storage by activated sludge. Water Sci Tech 45(6):157–168.

Beun JJ, Paletta F, van Loosdrecht MCM, Heijnen JJ. 2000. Stoichiometry and kinetics of poly-B-hydroxybutyrate metabolism in aerobic, slow growing activated sludge cultures. Biotechnol Bioeng 67:379–389.

Beun JJ, Dircks K, van Loosdrecht MCM, Heijnen JJ. 2002. Poly-B-hydroxybutyrate metabolism in dynamically fed mixed microbial cultures. Water Res 36:1167–1180.

Carucci A, Dionisi D, Majone M, Rolle E, Smurra P. 2001. Aerobic storage by activated sludge on real wastewater. Water Res 35:3833–3844.

Chudoba P, Capdeville B, Chudoba J. 1992. Explanation of biological meaning of the S0/X0 ratio in batch cultivation Water Sci Tech 26(3–4):743–751.

Comeau Y, Hall KJ, Oldham WK. 1988. Determination of poly-hydroxybutyrate and poly-hydroxyvalerate in activated sludge by gas–liquid chromatography. Appl Environ Microbiol 54:2325–2327

Dircks K, Henze M, van Loosdrecht MCM, Mosbaek H, Aspegren H. 2001. Storage and degradation of poly-B-hydroxybutyrate in activated sludge under aerobic conditions. Water Res 35:2277–2285.

Dochain D, Vanrolleghem PA. 2001. Dynamical modelling and estimation in wastewater treatment processes. London, UK: IWA Publishing.

Gernaey K, Petersen B, Nopens I, Comeau Y, Vanrolleghem PA. 2002a. Modelling aerobic carbon source degradation processes using titrimetric data and combined respirometric–titrimetric data: Experimental data and model structure. Biotechnol Bioeng 79:741–753.

Gernaey K, Petersen B, Dochain D, Vanrolleghem PA. 2002b. Modelling aerobic carbon source degradation processes using titrimetric data and combined respirometric–titrimetric data: Structural and practical identifiability. Biotechnol Bioeng 79:754–769.

Grady CPL, Jr., Smets BF, Barbeau DS. 1996. Variability in kinetic parameter estimates: A review of possible causes and a proposed terminology. Water Res 30:742–748.

Guisasola A, Baeza JA, Carrera J, Casas C, Lafuente J. 2003. An off-line respirometric procedure to determine inhibition and toxicity of biodegradable compounds in biomass from an industrial WWTP. Water Sci Tech 48(11–12):267–275.

Guisasola A, Pijuan M, Baeza JA, Carrera J, Casas C, Lafuente FJ. 2004a. Aerobic phosphorus release linked to acetate uptake in bio-P-sludge. Process modelling using oxygen uptake rate measurements. Biotechnol Bioeng 85(7):722–733.

Guisasola A, Sin G, Baeza JA, Carrera J, Vanrolleghem P. 2004b. Limitations of ASM1 and ASM3: A comparison based on batch OUR profiles from different full-scale WWTPs. In Proceedings 2nd IWA congress, Marrakech, Morocco, 19–24 September 2004.

Gujer W, Henze M, Takahashi M, van Loosdrecht MCM. 1999. Activated sludge model no. 3, Water Sci Tech 29(1):183–193.

Henze M, Gujer W, Mino T, van Loosdrecht MCM. 2000. Activated sludge models ASM1, ASM2, ASM2d, and ASM3. London: IWA Scientific and Technical Report no. 9 IWA.

Karahan-Gül Ö, van Loosdrecht MCM, Orhon D. 2003. Modification of activated sludge model no. 3 considering direct growth on primary substrate. Water Sci Tech 47(11):219–225.

Keesman KJ, Spanjers H, van Straten G. 1997. Analysis of endogenous process behaviour in activated sludge. Biotechnol Bioeng 57:155–163.

Koch G, Kühni M, Gujer W, Siegrist H. 2000. Calibration and validation of activated sludge model no. 3 for swiss municipal wastewater. Water Res 34:3580–3590.

Krishna C, van Loosdrecht MCM. 1999. Substrate flux into storage and growth in relation to activated sludge modelling. Water Res 33(14):3149–3161.

Lavallée B, Lessard P, Vanrolleghem P. 2005. Modeling the metabolic adaptations of the biomass under rapid growth and starvation conditions in the activated sludge process. J Environ Eng Sci (in press).

Nelder JA, Mead R. 1965. A simplex method for function minimization. Comput J 7:308–313.

Pratt S, Yuan Z, Keller J. 2003. Development of a novel titration and off-gas analysis (TOGA) sensor for study of biological processes in wastewater treatment systems. Biotechnol Bioeng 81:482–495.

Pratt S, Yuan Z, Keller J. 2004. Modelling aerobic carbon oxidation and storage by integrating respirometric, titrimetric, and off-gas CO$_2$ measurements. Biotechnol Bioeng 88:135–147.

Sin G. 2004. Systematic calibration of activated sludge models. PhD thesis. Faculty of Agricultural and Applied Biological Sciences. Ghent University. p 349.

Sin G, Malisse K, Vanrolleghem P. 2003. An integrated sensor for the monitoring of aerobic and anoxic activated sludge activities in biological nitrogen removal plants. Water Sci Tech 47(2):141–148.

Spanjers H, Vanrolleghem PA, Nguyen K, Vanhooren H, Patry GG. 1998. Towards a simulation-benchmark for evaluating respirometry-based control strategies. Water Sci Tech 37(12):219–226.

Van Aalst-van Leeuwen MA, Pot MA, van Loosdrecht MCM, Heijnen JJ. 1997. Kinetic modelling of poly(β-hydroxybutyrate) production and consumption by Paracoccus pantotrophus under dynamic substrate supply. Biotechnol Bioeng 55:773–782.

van Loosdrecht MCM, Heijnen JJ. 2002. Modelling of activated sludge processes with structured biomass. Water Sci Tech 45(6):12–23.

van Loosdrecht MCM, Pot MA, Heijnen JJ. 1997. Importance of bacterial storage polymers in bioprocesses. Water Sci Tech 35(1):41–47.

Vanrolleghem PA, Van Daele M, Dochain D. 1995. Practical identifiability of a biokinetic model of activated sludge respiration. Water Res 29:2561–2570.

Vanrolleghem PA, Gernaey K, Coen F, Petersen B, De Clerq B, Ottoy JP. 1998. Limitations of short-term experiments designed for identification of activated sludge biodegradation models by fast dynamic phenomena.

In Proceedings 7th IFAC Conference on Computer Applications in Biotechnology. Osaka, Japan. May 31–June 4, 1998.

Vanrolleghem P, Sin G, Gernaey K. 2004. Transient response of aerobic and anoxic activated sludge activities to sudden concentration changes. Biotechnol Bioeng 86:277–290.